VIBRATION ANALYSIS AND DAMPING CHARACTERISTICS OF HYBRID COMPOSITE PLATE USING FINITE ELEMENT ANALYSIS

A Thesis submitted in partial fulfillment of the Requirements for the degree of

Master of Technology
In
Mechanical Engineering
Specialization: Machine Design and Analysis

By
SHIVAPRASAD BAAD
Roll No. : 212ME1272

Department of Mechanical Engineering
National Institute of Technology Rourkela
Rourkela, Odisha, 769008, India
June 2014

VIBRATION ANALYSIS AND DAMPING CHARACTERISTICS OF HYBRID COMPOSITE PLATE USING FINITE ELEMENT ANALYSIS

A Thesis submitted in partial fulfillment of the Requirements for the degree of

Master of Technology
In
Mechanical Engineering
Specialization: Machine Design and Analysis

By
Shivaprasad Baad
Roll No. : 212ME1272

Under the Guidance of
Prof. Tarapada Roy

Department of Mechanical Engineering
National Institute of Technology Rourkela
Rourkela, Odisha, 769008, India
June 2014

Dedicated to…,

My parents, my sister

My maternal aunt and uncles

DEPT. OF MECHANICAL ENGINEERING
NATIONAL INSTITUTE OF TECHNOLOGY, ROURKELA
ROURKELA – 769008, ODISHA, INDIA

Certificate

This is to certify that the work in the thesis entitled **VIBRATION ANALYSIS AND DAMPING CHARACTERISTICS OF HYBRID COMPOSITE PLATE USING FINITE ELEMENT ANALYSIS** by **Shivaprasad Baad** is a record of an original research work carried out by her during 2013 - 2014 under my supervision and guidance in partial fulfillment of the requirements for the award of the degree of Master of Technology in Mechanical Engineering (Machine Design and Analysis), National Institute of Technology, Rourkela. Neither this thesis nor any part of it, to the best of my knowledge, has been submitted for any degree or diploma elsewhere.

Place: NIT Rourkela

Date: 02 June 2014

Professor

Dr. Tarapada Roy

DEPT. OF MECHANICAL ENGINEERING
NATIONAL INSTITUTE OF TECHNOLOGY, ROURKELA
ROURKELA – 769008, ODISHA, INDIA

Declaration

I certify that

a) The work contained in the thesis is original and has been done by myself under the general supervision of my supervisor.

b) The work has not been submitted to any other Institute for any degree or diploma.

c) I have followed the guidelines provided by the Institute in writing the thesis.

d) Whenever I have used materials (data, theoretical analysis, and text) from other sources, I have given due credit to them by citing them in the text of the thesis and giving their details in the references.

e) Whenever I have quoted written materials from other sources, I have put them under quotation marks and given due credit to the sources by citing them and giving required details in the references.

Shivaprasad Baad

2nd June 2014

ACKNOWLEDGEMENTS

It is my immense pleasure to avail this opportunity to express my gratitude, regards and heartfelt respect to Prof. Tarapada Roy, Department of Mechanical Engineering, NIT Rourkela for his endless and valuable guidance prior to, during and beyond the tenure of the project work. His priceless advices have always lighted up my path whenever I have struck a dead end in my work. It has been a rewarding experience working under his supervision as he has always delivered the correct proportion of appreciation and criticism to help me excel in my field of research.

I also express my sincere gratitude to Prof. (Dr.) K. P. Maity, Head of the Department of Mechanical Engineering for valuable departmental facilities.

I would like to make a special mention of the selfless support and guidance I received from my senior Ashirbad Swain, Ph.D. scholar, Department of Mechanical Engineering, NIT Rourkela during my project work.

Last but not the least; I would like to express my love, respect and gratitude to my parents, younger sister and my maternal aunt and uncles, who have always supported me in every decision I have made, guided me in every turn of my life, believed in me and my potential and without whom I would have never been able to achieve whatsoever I could have till date.

SHIVAPRASAD BAAD

shivaprasadbaad@gmail.com

ABSTRACT

Hybrid composite is a composite which consists of nanoparticles to enhance the strength as compared to conventional composites. A model has been proposed to determine the elastic properties of hybrid composite. The hybrid composite consists of conventional fiber and nanocomposite as matrix. The first step here is to determine the properties of nanocomposite which is done by using Mori – Tanaka method. The CNTs are considered as cylindrical inclusions in polymer matrix in Mori – Tanaka method. Assuming perfect bonding between carbon fibers and nanocomposite matrix, the effective properties of the hybrid composite has been evaluated using mechanics of materials approach.

An 8 noded shell element has been used for the finite element analysis having 5 degrees of freedom each node $(u, v, w, \theta_x, \theta_y)$. A 10×10 finite element mesh has been used to model the shell element. The shell coordinates which are in Cartesian form are converted into parametric form using two parameters (α_1, α_2). These parameters are again mapped into isoparametric form (η, ξ). A 16 layered laminate with stacking sequence $[0\ {-45}\ 45\ 90]_{2S}$ has been used for vibration analysis of simply supported shell element. The dynamic equations of shell are derived using Hamilton's principle. As the damping characters of the dynamic system are not available, for further investigation damping ratio of first mode and last active mode are assumed. Using Rayleigh damping the damping ratios of intermediate modes can be calculated. The time decay of the system from maximum amplitude to 5% of the maximum amplitude has been used as a parameter to study various shell structures by varying the volume fraction of CNTs in nanocomposite and by varying carbon fiber volume fraction.

CONTENTS

NOMENCLATURE

CNT	Carbon nanotubes
SWCNT	Single walled carbon nanotubes
DWCNT	Double walled carbon nanotubes
MWCNT	Multi walled carbon nanotubes
nc, m, hc	Nanocomposite, matrix, hybrid composite
C_{p11}, C_{p12}, C_{p22}, C_{p23}, C_{p55}	Elastic properties of constituent phase
n_r, k_r, p_r, l_r, m_r	Hills elastic constant
α, β	Euler angles for CNT orientation
σ, ε	Stress and strain
A	Strain concentration tensor
I	Identity matrix
S	Eshelby tensor
K	Bulk modulus
G	Shear modulus
E	Young's modulus
v_{CNT}	Volume fraction of CNT
v_m	Volume fraction of matrix
v_f	Volume fraction of fiber
α_1, α_2	Curvilinear coordinates
$s_{\alpha 1}, s_{\alpha 2}$	Isoparametric curves
r_1, r_2	Tangent to isoparametric curves
A_1, A_2	Lame's parameters
R_1, R_2	Normal curvatures of shell mid-surface
R_{12}	Twist curvatures of shell mid-surface
a	Length of shell along x-axis
N	Shape function
u_{0i}, v_{0i}, w_{0i}	Displacements of i^{th} node in α_1, α_2 and z directions
ξ, η	Isoparametric coordinates

J^*	Jacobian matrix
γ	Shear strain
k	Curvature of the mid-surface
B_b^e	In-plane strain displacement matrix
B_s^e	Transverse strain displacement matrix
N, M	Resultant force and moment per unit length
A	In-plane stiffness matrix
B	Coupling stiffness matrix
D	Bending stiffness matrix
z	Thickness of lamina
h	Thickness of laminate
Q	Reduced stiffness matrix
K	Shear correction factor
Π	Total potential energy
U	Strain energy
T	Kinetic energy
W	Work done by external force
L	Lagrangian
M_{uu}^e	Elemental mass matrix
K_{uu}^e	Elemental stiffness matrix
d_e	Displacement vector
$\ddot{d}^e$	Acceleration vector
t	Time
ρ	Density
ω	Natural frequency
ω^{**}	Non-dimensional natural frequency
γ_i	Modal coordinates for i^{th} degree of freedom
ζ_i	Modal damping ratio
$\chi_{1.....}\chi_{2n}$	State vector

LIST OF FIGURES

LIST OF TABLES

1

INTRODUCTION

As long as there is development in the field of aerospace, automobile, healthcare, electronics and consumer industry the demand for new materials will never seize. The demand for new materials has led to continuous research and development of new techniques to satisfy the needs.

1.1. Nanocomposites

Nanocomposites consist of reinforcements of nanoscale spread evenly or randomly in polymer matrix. The commonly used polymeric matrix materials are:

- Epoxy
- Nylon
- PEEK – Polyether ether ketone
- Polystyrene
- Polyimide

The commonly used nano fillers are:

- Carbon nanotubes – SWCNTs and MWCNTs
- Nanoaluminium oxide
- Nanotitanium oxide
- Nanosilica

The reinforcements can be particles or fibres of size of few nanometers. The nanocomposite has a wide range of materials from 3-D metal matrix composites, 2-D laminated composites and nano-wires of small dimension representing variations of nano reinforcements. Using nanoscale reinforcements was introduced by Usuki et al [1] who

built a nanocomposite using polyimide and organophilic clay. The nanocomposite formed had twice the tensile modulus as compared to neat polyimide with just 2% volume fraction of nano reinforcement. Nanocomposites have gained a wide popularity among researchers. Researchers have discovered that the properties of the nanocomposite are better when compared to the individual components of the composite. Properties such as increased tensile strength, increased thermal conductivity are observed.

1.2. Hybrid Composites

The important properties that are desired from any composite are strength, stiffness, ductility, toughness, damping, energy absorption, thermal stability and low weight. With conventional materials it is not possible to get all the desired properties, but with composite materials we can tailor the properties of material as per our needs. By using reinforcements of nanoscale in polymer composites there has been tremendous increase in mechanical properties as compared to neat polymer matrix. Hybrid composites are new type of three phase composites which have reinforcements of nanoscale in addition to conventional reinforcing fiber in matrix or by growing reinforcements of nanoscale on the surface of fiber. R.C.L. Dutra et al [2] defined hybrid composites as composites consisting of different fibers. The main purpose of using hybrid composites is it increases the matrix dominated properties.

1.3. Classification of Plates [3]

Plates can be classified into two types:

- Thin plates
- Thick plates

A thin plate can further be classified as:

- Plate with small deflection
- Plates with large deflection

1.3.1.1. Plates with small deflection

If the deflection of a plate when subjected to loading is less than or nearly equal to thickness, then the plate is said to have small deflection. The necessary assumptions for developing theory for plates having small deflection are:

- The middle plane does not deform on loading.
- Point on the plate initially normal to middle plane remain normal to middle plane even after loading.
- The stresses in the thickness direction can be neglected.

1.3.1.2. Thin plates with large deflection

If the deflections of the plate are large when subjected to lateral loading as compared to thickness, then the plate is said to have large deflection. When plate is loaded mid plane strains are developed. In plates with small deflection it is normally neglected, as a result the stresses are also neglected. But if deflections are large as compared to thickness, the strains developed are large. So stresses cannot be neglected. In this case we obtain nonlinear equations and analysis becomes complicated.

1.3.2. Thick plate

The above approximations for thin plates are not applicable. Thick plate theory must be used. The thick plate theory involves 3-D theory of elasticity and calculation of stresses is quite complicated.

1.3.3. Difference between plate and shell

- The major difference between plates and shells can be observed under the action of loading. When a plate member is subjected to lateral load, equilibrium is possible by the action of bending and twisting moments. In shells, when it is subjected to lateral loading, equilibrium is possible by membrane stresses which act parallel to tangential plane at a point on middle surface and are distributed uniformly over the thickness of shell.
- Plates are plane member and shells are curved structural members.

1.4 Damping in composites

Damping is a very important parameter for vibration control, noise reduction, stability of system, fatigue and impact resistance [4]. The damping in fibre reinforced composites is different from that of metals.

The various forms of energy dissipation are [5]:

- Damping behaviour of matrix material.

  The major contribution to damping is from matrix, the damping of fiber must also be included for calculation of damping.

- Damping behaviour of interphase

  Interphase is the region between matrix and fiber. The type of interphase plays an important role in damping. The interphase can be weak or strong.

- Damping due to damage
    a) Frictional damping due to delamination.
    b) Damping due to energy dissipation of broken fibers or cracks in matrix.
- Viscoplastic damping

    At higher amplitudes of stresses, there is non-linear damping due to presence of high stress and strain.

1.5. Impulse response of linear time invariant system (LTIS)

Impulse force is a force which acts on the system for very short amount of time. Knowing the impulse response of LTIS we can obtain by superposition the response of the same system to any input provided the input conditions are zero in all cases. Unit impulse input has very short intervals of time but very large amplitude and hence the effect of the behaviour of the system under study is not negligible. Ex: Ball hitting the cricket bat, the ball is acted upon by very large force for a short duration of time.

2

LITERATURE REVIEW AND MOTIVATION

2.1 Literature Review

Jian Ping Lu [6] Elastic properties of SWCNTs, MWCNTs and nanoropes are investigated using force constant model.

2.1.1 Material property – Hybrid composite

Raifee et al [7] estimated mechanical properties of epoxy based nanocomposite with SWCNT, MWCNT and graphene platelets were compared for weight fractions of 0.1%. The material properties measured were Young's modulus, fracture toughness, ultimate tensile strength. The tensile strength of graphene based nanocomposites showed better properties as compared to CNT based nanocomposites. F.H. Gojny et al [8] observed mechanical properties resulted in an increase in Young's modulus, strength at weight fractions of 0.1%. There was good agreement between experimental observed data and results from modified Halpin-Tsai relation. Florian H [9] proposed choosing appropriate type of CNTs (SWCNTs or DWCNTs or MWCNTs) has been a problem ever since they are being used in composites. They evaluated the properties of nanocomposite for different nano fillers. The nanocomposites exhibited greater strength, stiffness and fracture toughness. They found that DWCNT based nanocomposite exhibited greater fracture toughness. Seidel et al [10] estimated effective elastic properties of composites consisting of aligned SWCNTs or MWCNTs using Mori-Tanaka method. The effects of an interphase layer between CNTs and the polymer is also investigated using a multi-layer composite cylinders approach. Liu and Chen [11] estimated effective elastic properties of the nanocomposite are evaluated using continuum modelling and finite element method. The extended rule of mixture is used to determine the properties of the continuum model.

2.1.2 Material Property – Hybrid composite

Dutra et al [2], made a hybrid composite consisting of carbon fiber and Polypropylene fiber and mercapto-modified polypropylene blend fiber (PPEVASH). They found that hybrid composites showed better impact resistance than CFRP composite. Mathur et al [12] CNTs were grown on unidirectional carbon fiber. These fibers were used as reinforcements in matrix material. They found that the mechanical properties improved with increase in amount of CNT deposition as compared to neat CFRP composite. Garcia et al [13] CNTs were grown on alumina fiber cloth. These fibers were used as reinforcements in matrix material. The growth of CNTs led to an increase in inter-laminar shear properties of the order of 69% as compared to alumina cloth composite. Kundalwal and Ray [14], they evaluated the elastic properties of FFRC (Fuzzy fiber reinforced composite) using mechanics of materials approach and Mori-Tanaka method considering with and without the interphase between CNT and polymer.

2.1.3 Vibration analysis of plate

Roy and Chakraborty [15] formulated layered shell finite element model for coupled electromechanical analysis of curved smart composite structure.

2.1.4 Damping in composites

Gibson et al [4] used vibration used modal vibration response measurements to characterize the mechanical properties of laminated structures. They showed that vibration in either first mode or multiple modes can be used to determine the elastic properties and damping ratios. Modal testing was done by impulse excitation methods. Kyriazoglou and Guild [17] found damping ratio using experimental methods and by FEM. The FEM uses Rayleigh damping method and particularly mass proportional damping. R. Verdejoan et al. [18] found that even a small volume fraction of CNT can increase the sound absorption capabilities.

2.2 Motivation

Hybrid composites are new type of three phase composites which increase the matrix dominated properties. The hybrid composite that is to be modeled here consists of nanocomposite matrix and continuous long carbon fibers. The nanocomposite is made up of randomly distributed CNTs and polymer matrix. The nanocomposite is modeled using Mori-Tanaka method. The hybrid composite can be modeled using mechanics of materials approach. As the mobility of system goes on increasing, modeling damping for such systems becomes complicated. Rayleigh damping model has been used to model such multi degree of freedom systems. Further investigation has been carried out by assuming suitable damping ratios for first mode and last significant mode where

mass is proportional to damping. Impulse response of the system has been carried out and a comparative study has been made to know effect of damping in systems by varying the volume fractions of carbon fiber and CNTs.

2.3 Objective

- Material modelling and material characterization
    1. Nanocomposite has been modelled using Mori – Tanaka method.
    2. Hybrid composite consisting of carbon fiber and nanocomposite matrix has been modelled using mechanics of materials approach.
- 8 noded shell element formulation
    1. Mindlin theory of plates and shells has been used to model shell.
- Modelling damping and Impulse response
    1. Rayleigh damping has been used to model the damping of MDOF system.
    2. Impulse response of the system has been carried out using the state space model.

3

MATERIAL MODELING

The material modeling is divided in two phases:

- CNT based nanocomposite modeling.
- Hybrid composite modeling.

The nanocomposite consists of randomly distributed straight MWCNT as reinforcements and epoxy as matrix. As the CNTs are randomly distributed the nanocomposite can be modeled as isotropic material. The property of nanocomposite is evaluated using the Mori – Tanaka method. Assuming perfect bonding between fiber and nanocomposite the hybrid composite can be modeled similar to conventional composite using mechanics of materials approach.

3.1 CNT bases nanocomposite modeling

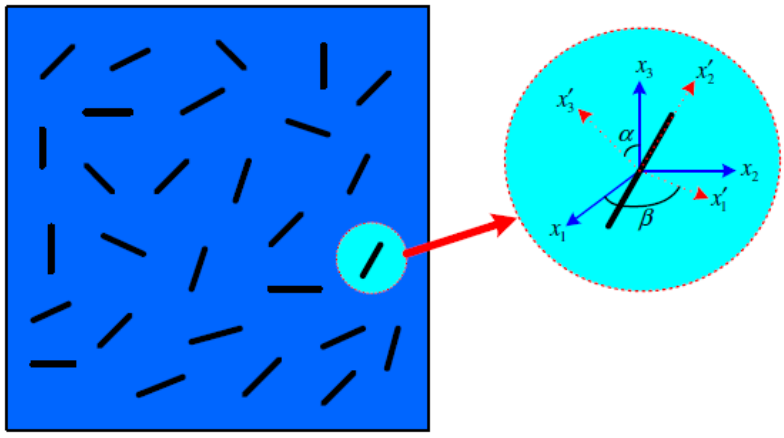

FIGURE 3-1 REF: HESHMATI AND YAS [18]

Fig. 3.1 shows a RVE of randomly distributed CNT in epoxy matrix.

The Mori – Tanaka method was used to estimate the elastic properties of the randomly distributed MWCNT in matrix. The procedure to determine the isotropic properties of randomly oriented MWCNTs dispersed in epoxy matrix is as follows:

- The Hill's elastic constants for the MWCNT can be obtained by equating the stress – strain matrix of MWCNT with the Hill's elastic matrix.

$$\left[C_{CNT}\right]=\begin{bmatrix} C_{11}^{CNT} & C_{12}^{CNT} & C_{13}^{CNT} & 0 & 0 & 0 \\ C_{21}^{CNT} & C_{22}^{CNT} & C_{23}^{CNT} & 0 & 0 & 0 \\ C_{31}^{CNT} & C_{32}^{CNT} & C_{33}^{CNT} & 0 & 0 & 0 \\ 0 & 0 & 0 & C_{44}^{CNT} & 0 & 0 \\ 0 & 0 & 0 & 0 & C_{55}^{CNT} & 0 \\ 0 & 0 & 0 & 0 & 0 & C_{66}^{CNT} \end{bmatrix} \quad (1)$$

$$\left[C_{CNT}\right]=\begin{bmatrix} n_r & l_r & l_r & 0 & 0 & 0 \\ l_r & k_r+m_r & k_r-m_r & 0 & 0 & 0 \\ l_r & k_r-m_r & k_r+m_r & 0 & 0 & 0 \\ 0 & 0 & 0 & m_r & 0 & 0 \\ 0 & 0 & 0 & 0 & p_r & 0 \\ 0 & 0 & 0 & 0 & 0 & p_r \end{bmatrix} \quad (2)$$

Eqn (1) and eqn. (2) are the stress – strain matrix of MWCNT and Hill's elastic matrix.

The orientation of the CNT can be specified by two Euler angles α and β. The base vectors e_i and e_i' of the global $\left(0-x_1x_2x_3\right)$ and local co-ordinates can be related by the relation,

$$e_i = g_{ij}e_j' \quad (3)$$

Where $g_{ij}=\begin{bmatrix} \cos\beta & -\cos\alpha\sin\beta & \sin\alpha\sin\beta \\ \sin\beta & \cos\alpha\cos\beta & -\sin\alpha\cos\beta \\ 0 & \sin\alpha & \cos\alpha \end{bmatrix}$

- As the CNTs are randomly distributed in matrix it can be characterized by two Euler angles α and β. The orientation distribution of CNTs in the composite is characterized by the probability density function $p(\alpha,\beta)$ satisfying the normalization condition and is given by the equation.

$$\int_0^{2\pi}\int_0^{\pi/2} p(\alpha,\beta)\sin\alpha(d\alpha)(d\beta)=1 \quad (4)$$

- For completely randomly oriented CNTs,

$$p(\alpha,\beta)=\frac{1}{2\pi} \quad (5)$$

- From Mori – Tanaka method one can relate stress $\sigma_{CNT}(\alpha,\beta)$ and strain $\varepsilon_{CNT}(\alpha,\beta)$ of the CNT to the stress in the matrix σ_m by,

$$\sigma_{CNT}(\alpha,\beta)=C_{CNT}A(\alpha,\beta)\varepsilon_m=\left[C_{CNT}A(\alpha,\beta)C_m^{-1}\right]\sigma_m \quad (6)$$

And

$$\varepsilon_{CNT}(\alpha,\beta) = A(\alpha,\beta)\varepsilon_m = \left[A(\alpha,\beta)C_m^{-1}\right]\sigma_m \tag{7}$$

Where strain concentration tensor is given by,

$$A = \left[I + S(C_m)^{-1}(C_{CNT} - C_m)\right]^{-1} \tag{8}$$

Where S corresponds to Eshelby Tensor and is given by Li and Dunn [19] for cylindrical inclusion. The average stress and strain for the randomly oriented CNTs is given by,

$$\sigma_{CNT} = \left[\int_0^{2\pi}\int_0^{\pi/2} p(\alpha,\beta)\left[C_{CNT}A(\alpha,\beta)C_m^{-1}\right]\sin\alpha d\alpha d\beta\right]\sigma_m \tag{9}$$

$$\varepsilon_{CNT} = \left[\int_0^{2\pi}\int_0^{\pi/2} p(\alpha,\beta)A(\alpha,\beta)\sin\alpha d\alpha d\beta\right]\varepsilon_m \tag{10}$$

Using rule of mixture one can get the stresses and strains in the nanocomposite.

As the CNTs are randomly distributed in the matrix, the nanocomposite behaves like an isotropic material. The bulk modulus, shear modulus, Young's modulus of the nanocomposite [20] are given by,

$$\begin{aligned} K_{nc} &= K_m + \frac{v_{CNT}(\delta_{CNT} - 3K_m\alpha_{CNT})}{3(v_m + v_{CNT}\alpha_{CNT})} \\ G_{nc} &= G_m + \frac{v_{CNT}(\eta_{CNT} - 2G_m\beta_{CNT})}{2(v_m + v_{CNT}\beta_{CNT})} \\ E_{nc} &= \frac{9K_{nc}G_{nc}}{3K_{nc} + G_{nc}} \end{aligned} \tag{11}$$

Where,

$$\begin{aligned} \alpha_{CNT} &= \frac{3(K_m + G_m) + k_{CNT} - l_{CNT}}{3(G_m + k_{CNT})} \\ \beta_{CNT} &= \frac{1}{5}\left\{\frac{4G_m + 2k_{CNT} + l_{CNT}}{3(G_m + k_{CNT})} + \frac{4G_m}{G_m + p_{CNT}} + \frac{2\left[G_m(3K_m + G_m) + G_m(3K_m + 7G_m)\right]}{G_m(3K_m + G_m) + m_{CNT}(3K_m + 7G_m)}\right\} \\ \delta_{CNT} &= \frac{1}{3}\left[n_{CNT} + 2l_{CNT} + \frac{(2k_{CNT} + l_{CNT})(3K_m + 2G_m - l_{CNT})}{G_m + k_{CNT}}\right] \\ \eta_{CNT} &= \frac{1}{5}\left[\frac{2}{3}(n_{CNT} - l_{CNT}) + \frac{8G_m p_{CNT}}{G_m + p_{CNT}} + \frac{8G_m m_{CNT}(3K_m + 4G_m)}{3K_m(m_{CNT} + G_m) + G_m(7m_{CNT} + G_m)} + \frac{2(k_{CNT} - l_{CNT})(2G_m + l_{CNT})}{3(G_m + k_{CNT})}\right] \end{aligned} \tag{12}$$

$$v_{CNT} + v_m = 1 \tag{13}$$

v_{CNT} and v_m are volume fractions of CNT and matrix material, *nc* represents nanocomposite.

3.2 Hybrid Composite modeling

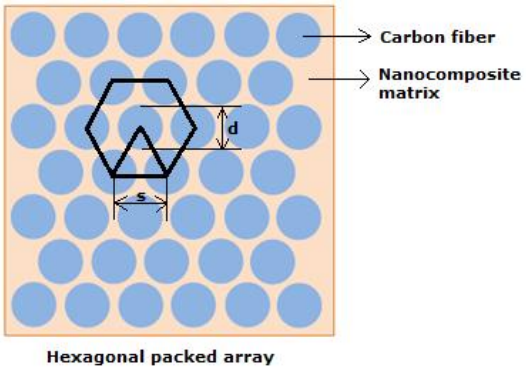

FIGURE 3-2 HEXAGONAL RVE

Fig. 3.2 shows a hexagonal RVE of hybrid composite consisting of carbon fibers distributed in nanocomposite matrix.

- Using the above calculated nanocomposite properties, the properties of the transversely isotropic hybrid composite can be evaluated by the formulation of Kundalwal and Ray for fuzzy fiber [14].
- Assuming perfect bonding between carbon fiber and nanocompostie, the normal strains in hybrid composite, carbon fiber and nanocomposite are equal along the fiber direction and the transverse stresses in the same phase are equal along the direction transverse to the fiber from isofield conditions.
- Using rules of mixture one can express the longitudinal and transverse stresses and strains in terms of volume fractions of nanocomposite and carbon fiber.
- Using isofield conditions and rule of mixture we can write,

$$v_f + v_{NC} = 1 \tag{14}$$

Where v_f and v_{NC} are volume fractions of carbon fiber and nanocomposite.

$$\begin{Bmatrix} \varepsilon_1^f \\ \sigma_2^f \\ \sigma_3^f \\ \sigma_{23}^f \\ \sigma_{13}^f \\ \sigma_{12}^f \end{Bmatrix} = \begin{Bmatrix} \varepsilon_1^{NC} \\ \sigma_2^{NC} \\ \sigma_3^{NC} \\ \sigma_{23}^{NC} \\ \sigma_{13}^{NC} \\ \sigma_{12}^{NC} \end{Bmatrix} = \begin{Bmatrix} \varepsilon_1^{HC} \\ \sigma_2^{HC} \\ \sigma_3^{HC} \\ \sigma_{23}^{HC} \\ \sigma_{13}^{HC} \\ \sigma_{12}^{HC} \end{Bmatrix} \tag{15}$$

HC represents hybrid composite.

$$v_f \begin{Bmatrix} \sigma_1^f \\ \varepsilon_2^f \\ \varepsilon_3^f \\ \varepsilon_{23}^f \\ \varepsilon_{13}^f \\ \varepsilon_{12}^f \end{Bmatrix} + v_{NC} \begin{Bmatrix} \sigma_1^{NC} \\ \varepsilon_2^{NC} \\ \varepsilon_3^{NC} \\ \varepsilon_{23}^{NC} \\ \varepsilon_{13}^{NC} \\ \varepsilon_{12}^{NC} \end{Bmatrix} = \begin{Bmatrix} \sigma_1^{HC} \\ \varepsilon_2^{HC} \\ \varepsilon_3^{HC} \\ \varepsilon_{23}^{HC} \\ \varepsilon_{13}^{HC} \\ \varepsilon_{12}^{HC} \end{Bmatrix} \tag{16}$$

There the stress and strain in the hybrid composite lamina is given by,

$$\left\{\sigma^{HC}\right\}=\left[C_1\right]\left\{\varepsilon^{f}\right\}+\left[C_2\right]\left\{\varepsilon^{NC}\right\} \tag{17}$$

$$\left\{\varepsilon^{HC}\right\}=\left[V_1\right]\left\{\varepsilon^{f}\right\}+\left[V_2\right]\left\{\varepsilon^{NC}\right\} \tag{18}$$

But from iso-field conditions,

$$\left[C_3\right]\left\{\varepsilon^{f}\right\}-\left[C_4\right]\left\{\varepsilon^{NC}\right\}=0 \tag{19}$$

By solving above equations we get,

$$\left\{\sigma^{HC}\right\}=\left[C^{HC}\right]\left\{\varepsilon^{HC}\right\} \tag{20}$$

$\left[C^{HC}\right]$ is the effective elastic matrix of the proposed Carbon fiber is reinforced polymer and is given by,

$$\left[C^{HC}\right]=\left[C_1\right]\left[V_3\right]^{-1}+\left[C_2\right]\left[V_4\right]^{-1} \tag{21}$$

The various matrices appearing in the above equations are given below.

$$\left[C_1\right]=v_f\begin{bmatrix} C_{11}^{f} & C_{12}^{f} & C_{12}^{f} & 0 & 0 & 0 \\ 0 & 0 & 0 & 0 & 0 & 0 \\ 0 & 0 & 0 & 0 & 0 & 0 \\ 0 & 0 & 0 & 0 & 0 & 0 \\ 0 & 0 & 0 & 0 & 0 & 0 \\ 0 & 0 & 0 & 0 & 0 & 0 \end{bmatrix} \tag{22}$$

$$\left[C_2\right]=\begin{bmatrix} v_{NC}C_{11}^{NC} & v_{NC}C_{12}^{NC} & v_{NC}C_{12}^{NC} & 0 & 0 & 0 \\ C_{12}^{NC} & C_{11}^{NC} & C_{12}^{NC} & 0 & 0 & 0 \\ C_{12}^{NC} & C_{12}^{NC} & C_{11}^{NC} & 0 & 0 & 0 \\ 0 & 0 & 0 & C_{44}^{NC} & 0 & 0 \\ 0 & 0 & 0 & 0 & C_{44}^{NC} & 0 \\ 0 & 0 & 0 & 0 & 0 & C_{44}^{NC} \end{bmatrix} \tag{23}$$

$$\left[C_3\right]=\begin{bmatrix} 1 & 0 & 0 & 0 & 0 & 0 \\ C_{12}^{f} & C_{22}^{f} & C_{23}^{f} & 0 & 0 & 0 \\ C_{13}^{f} & C_{23}^{f} & C_{22}^{f} & 0 & 0 & 0 \\ 0 & 0 & 0 & C_{44}^{p} & 0 & 0 \\ 0 & 0 & 0 & 0 & C_{55}^{p} & 0 \\ 0 & 0 & 0 & 0 & 0 & C_{55}^{p} \end{bmatrix} \tag{24}$$

$$[C_4]=\begin{bmatrix} 1 & 0 & 0 & 0 & 0 & 0 \\ C_{12}^{NC} & C_{11}^{NC} & C_{12}^{NC} & 0 & 0 & 0 \\ C_{12}^{NC} & C_{12}^{NC} & C_{11}^{NC} & 0 & 0 & 0 \\ 0 & 0 & 0 & C_{44}^{NC} & 0 & 0 \\ 0 & 0 & 0 & 0 & C_{44}^{NC} & 0 \\ 0 & 0 & 0 & 0 & 0 & C_{44}^{NC} \end{bmatrix} \tag{25}$$

$$[V_1]=\begin{bmatrix} 0 & 0 & 0 & 0 & 0 & 0 \\ 0 & v_f & 0 & 0 & 0 & 0 \\ 0 & 0 & v_f & 0 & 0 & 0 \\ 0 & 0 & 0 & v_f & 0 & 0 \\ 0 & 0 & 0 & 0 & v_f & 0 \\ 0 & 0 & 0 & 0 & 0 & v_f \end{bmatrix} \tag{26}$$

$$[V_2]=\begin{bmatrix} 1 & 0 & 0 & 0 & 0 & 0 \\ 0 & v_{NC} & 0 & 0 & 0 & 0 \\ 0 & 0 & v_{NC} & 0 & 0 & 0 \\ 0 & 0 & 0 & v_{NC} & 0 & 0 \\ 0 & 0 & 0 & 0 & v_{NC} & 0 \\ 0 & 0 & 0 & 0 & 0 & v_{NC} \end{bmatrix} \tag{27}$$

$$[V_3]=[V_1]+[V_2][C_4]^{-1}[C_3] \tag{28}$$

$$[V_4]=[V_2]+[V_1][C_3]^{-1}[C_4] \tag{29}$$

4

FINITE ELEMENT FORMULATION

4.1 Geometry of mid-surface of shell

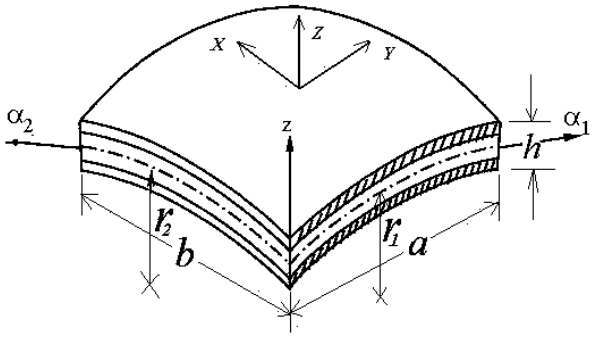

FIGURE 4-1 GEOMETRY OF SHELL STRUCTURE IN CARTESIAN COORDINATES

The shell geometry used in the present formulation has been developed using an orthogonal curvilinear coordinate system with the mid-plane of the shell assumed to be the reference surface as shown in Fig.4.1. The shell mid-surface in the Cartesian rectangular coordinate system has been first mapped into a parametric domain through the suitable exact parameterization. Two independent coordinates (α_1, α_2) in the parametric space have been considered as the mid-surface curvilinear coordinates of the shell. The normal direction coordinate to the middle surface of the shell has been represented by z. The reference surface or the shell mid-surface can be described in the global Cartesian coordinates in terms of the position vector as,

$$r(\alpha_1,\alpha_2) = X(\alpha_1,\alpha_2)\hat{i} + Y(\alpha_1,\alpha_2)\hat{j} + Z(\alpha_1,\alpha_2)\hat{k} \tag{30}$$

Where, $\hat{i}$, $\hat{j}$ and $\hat{k}$ are unit vectors along the *X*, *Y* and *Z* axis, respectively.

The tangent to the isoparametric curves $s_{\alpha 1}$ and $s_{\alpha 2}$ respectively are

$$r_1 = \frac{\partial r}{\partial \alpha_1}; \qquad r_2 = \frac{\partial r}{\partial \alpha_2} \tag{31}$$

The vector joining two points on the middle surface (α_1, α_2) and $(\alpha_1 + d\alpha_1, \alpha_2 + d\alpha_2)$ is given as

$$ds = r_1 d\alpha_1 + r_2 d\alpha_2 \tag{32}$$

Scalar product of *ds*,

$$ds.ds = (r_1.r_1)d\alpha_1^2 + (r_2.r_2)d\alpha_2^2 \tag{33}$$

Lame's parameters can be defined as,

$$\begin{aligned} A_1 &= \sqrt{r_1.r_1} \\ A_2 &= \sqrt{r_2.r_2} \end{aligned} \tag{34}$$

Eqn. (4) can be written as

$$ds^2 = A_1^{\,2} d\alpha_1^{\,2} + A_2^{\,2} d\alpha_2^{\,2} \tag{35}$$

Since the α_1 and α_2 are independent coordinates

$$ds^2 = ds_{\alpha 1}^2 + ds_{\alpha 2}^2 \tag{36}$$

Where, $\begin{aligned} ds_{\alpha 1} &= A_1 d\alpha_1 \\ ds_{\alpha 2} &= A_2 d\alpha_2 \end{aligned}$

The unit tangent vectors to the isoparametric curve $s_{\alpha 1}$ and $s_{\alpha 2}$ can be expressed respectively as,

$$\hat{e_1} = \frac{r_1}{A_1}; \qquad \hat{e_2} = \frac{r_2}{A_2} \tag{37}$$

The unit normal vector to the tangent plane of any point on the reference surface can be expressed as

$$\hat{e_n} = \frac{r_1 \times r_2}{|r_1 \times r_2|} \tag{38}$$

The normal curvatures and twist curvatures of the mid-surface of shell can be expressed as:

$$\begin{aligned} \frac{1}{R_1} &= -\frac{\hat{e_n}.r_{11}}{A_1^{\,2}} \\ \frac{1}{R_2} &= -\frac{\hat{e_n}.r_{22}}{A_2^{\,2}} \\ \frac{1}{R_{12}} &= -\frac{\hat{e_n}.r_{12}}{A_1 A_2} \end{aligned} \tag{39}$$

Where R_1, R_2 are the normal curvatures of the midsurface of the shell and R_{12} is the twist curvature of the mid-surface of the shell.

4.1.1 Isoparametric mapping

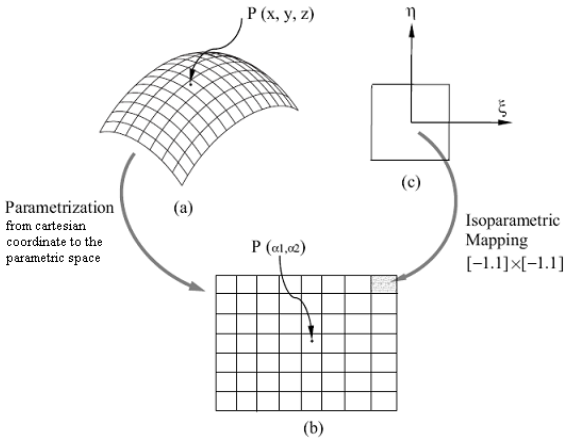

FIGURE 4-2 ISOPARAMETRIC MAPPING

Fig.4.2 shows Cartesian coordinates are converted into curvilinear coordinates and it is mapped into isoparametric form.

The shell midsurface in the rectangular cartesian coordinate system has been mapped into the parametric space (α_1, α_2) and the midsurface in the parametric space has been divided into required number of quadrilateral elements or sub-domains. The reference coordinates (ξ, η) map the quadrilateral element in the curvilinear coordinates (α_1, α_2) into the reference coordinates that is a square as shown in Fig. 4.2. Any point within an element in the parametric space has been approximated by the isoparametric mapping.

Hence the curvilinear coordinates (α_1, α_2) of any point within an element may be expressed as

$$\alpha_1 = \sum_{i=1}^{nd} N_i \alpha_{1i}$$
$$\alpha_2 = \sum_{i=1}^{nd} N_i \alpha_{2i} \qquad (40)$$

(α_1, α_2) is the coordinate of midsurface at i^{th} node in curvilinear coordinate system. u_{0i}, v_{0i} and w_{0i} are the deflection of midsurface at i^{th} node in α_1, α_2 and z directions respectively. θ_{1i} is the rotation of normal at i^{th} node about α_2 axis and θ_{2i} is the rotation of normal at i^{th} node about α_1 axis.

The displacement components on the shell midsurface at any point within an element may be expressed as

$$\begin{Bmatrix} u_0 \\ v_0 \\ w \\ \theta_1 \\ \theta_2 \end{Bmatrix} = \sum_{i=1}^{nd} N_i \begin{Bmatrix} u_{0i} \\ v_{0i} \\ w_i \\ \theta_{1i} \\ \theta_{2i} \end{Bmatrix} \tag{41}$$

Where, nd is the number of nodes in an element, N_i is the shape function corresponding to the i^{th} node and shape functions of 8 noded serendipity element are given below

$$\begin{aligned}
N_1 &= \frac{1}{4}(1-\xi)(1-\eta)(-1-\xi-\eta) \\
N_2 &= \frac{1}{2}(1-\xi^2)(1-\eta) \\
N_3 &= \frac{1}{4}(1+\xi)(1-\eta)(-1+\xi-\eta) \\
N_4 &= \frac{1}{2}(1+\xi)(1-\eta^2) \\
N_5 &= \frac{1}{4}(1+\xi)(1+\eta)(-1+\xi+\eta) \\
N_6 &= \frac{1}{2}(1-\xi^2)(1+\eta) \\
N_7 &= \frac{1}{4}(1-\xi)(1+\eta)(-1-\xi+\eta) \\
N_8 &= \frac{1}{2}(1-\xi)(1-\eta^2)
\end{aligned} \tag{42}$$

4.1.2 Transformation matrix used for isoparametric mapping

Since the integration is to be done in natural coordinates (ξ,η), the element is mapped into the isoparametric space (ξ,η) using the isoparametric shape functions. The transformation matrix used is given below.

The relation between the shape function derivatives in parametric space (α_1,α_2) and in isoparametric space (ξ,η) are given as

$$\begin{Bmatrix} \frac{\partial N_i}{\partial \alpha_1} \\ \frac{\partial N_i}{\partial \alpha_2} \end{Bmatrix} = \left[J^* \right]^{-1} \begin{Bmatrix} \frac{\partial N_i}{\partial \xi} \\ \frac{\partial N_i}{\partial \eta} \end{Bmatrix} \tag{43}$$

The jacobian matrix can be expressed as

$$\left[J^*\right]=\begin{bmatrix}\frac{\partial\alpha_1}{\partial\xi} & \frac{\partial\alpha_2}{\partial\xi}\\ \frac{\partial\alpha_1}{\partial\eta} & \frac{\partial\alpha_2}{\partial\eta}\end{bmatrix} \tag{44}$$

$$\left|J\right|=\sqrt{a}\left|J^*\right| \tag{45}$$

$$d\Omega=\left|J\right|d\xi d\eta \tag{46}$$

4.2 Strain displacement relations

Neglecting normal strain component in the thickness direction, the five strain components of a doubly curved shell may be express as

$$\begin{bmatrix}\varepsilon_{xx}\\ \varepsilon_{yy}\\ \gamma_{xy}\\ \gamma_{yz}\\ \gamma_{xz}\end{bmatrix}=\begin{bmatrix}\varepsilon^0_{xx}\\ \varepsilon^0_{yy}\\ \gamma^0_{xy}\\ \gamma^0_{yz}\\ \gamma^0_{xz}\end{bmatrix}+z\begin{bmatrix}k_{xx}\\ k_{yy}\\ k_{xy}\\ 0\\ 0\end{bmatrix} \tag{47}$$

Where $\varepsilon^0_{xx},\varepsilon^0_{yy}$ and γ^0_{xy} is the in-plane strains of the midsurface in the cartesian coordinate system and k_{xx},k_{yy} and k_{xy} are the bending strains (curvatures) of the midsurface in the cartesian coordinates system. After incorporating the effect of transverse stain in Koiter's shell theory, inplane and transverse strain-displacement relations may be expressed as described in the following subsections.

4.2.1 In-plane/bending strain-displacement matrix

The strain components on the midsurface of shell element are

$$\left\{\varepsilon\right\}=\begin{bmatrix}\varepsilon^0_{xx} & \varepsilon^0_{yy} & \gamma^0_{xy} & k_{xx} & k_{yy} & k_{xy}\end{bmatrix}^T \tag{48}$$

By using isoparametric 8-noded shell element, the displacement component on the shell midsurface at any point within an element can be expressed as

$$\begin{Bmatrix}u_0\\ v_0\\ w\\ \theta_1\\ \theta_2\end{Bmatrix}=\left[N\right]\left\{d^e\right\} \tag{49}$$

The mid-surface strains and curvatures from Koiter's shell theory are:

$$\varepsilon_{xx}^{0}=\frac{1}{A_1}\frac{\partial u}{\partial \alpha_1}+\frac{v}{A_1A_2}\frac{\partial A_1}{\partial \alpha_2}+\frac{w}{R_1} \tag{50}$$

$$\varepsilon_{yy}^{0}=\frac{1}{A_2}\frac{\partial v}{\partial \alpha_2}+\frac{u}{A_1A_2}\frac{\partial A_2}{\partial \alpha_1}+\frac{w}{R_2} \tag{51}$$

$$\gamma_{xy}^{0}=\frac{1}{A_1}\frac{\partial v}{\partial \alpha_1}+\frac{1}{A_2}\frac{\partial u}{\partial \alpha_2}-\frac{u}{A_1A_2}\frac{\partial A_1}{\partial \alpha_2}-\frac{v}{A_1A_2}\frac{\partial A_2}{\partial \alpha_1}+\frac{2w}{R_{12}} \tag{52}$$

$$k_{xx}=\frac{1}{A_1}\frac{\partial \theta_1}{\partial \alpha_1}+\frac{\theta_2}{A_1A_2}\frac{\partial A_1}{\partial \alpha_2}+\frac{1}{2R_{12}}\left(\frac{1}{A_1}\frac{\partial v}{\partial \alpha_1}-\frac{1}{A_2}\frac{\partial u}{\partial \alpha_2}-\frac{u}{A_1A_2}\frac{\partial A_1}{\partial \alpha_2}+\frac{v}{A_1A_2}\frac{\partial A_2}{\partial \alpha_1}\right) \tag{53}$$

$$k_{yy}=\frac{1}{A_2}\frac{\partial \theta_2}{\partial \alpha_2}+\frac{\theta_1}{A_1A_2}\frac{\partial A_2}{\partial \alpha_1}-\frac{1}{2R_{12}}\left(\frac{1}{A_1}\frac{\partial v}{\partial \alpha_1}-\frac{1}{A_2}\frac{\partial u}{\partial \alpha_2}-\frac{u}{A_1A_2}\frac{\partial A_1}{\partial \alpha_2}+\frac{v}{A_1A_2}\frac{\partial A_2}{\partial \alpha_1}\right) \tag{54}$$

$$k_{xy}=\begin{bmatrix}\dfrac{1}{A_1}\dfrac{\partial \theta_2}{\partial \alpha_1}+\dfrac{1}{A_2}\dfrac{\partial \theta_1}{\partial \alpha_2}-\dfrac{\theta_1}{A_1A_2}\dfrac{\partial A_1}{\partial \alpha_2}-\dfrac{\theta_2}{A_1A_2}\dfrac{\partial A_2}{\partial \alpha_1}- \\ \dfrac{1}{2}\left(\dfrac{1}{R_1}-\dfrac{1}{R_2}\right)\left(\dfrac{1}{A_1}\dfrac{\partial v}{\partial \alpha_1}-\dfrac{1}{A_2}\dfrac{\partial u}{\partial \alpha_2}-\dfrac{u}{A_1A_2}\dfrac{\partial A_1}{\partial \alpha_2}+\dfrac{v}{A_1A_2}\dfrac{\partial A_2}{\partial \alpha_1}\right)\end{bmatrix} \tag{55}$$

By using 8-noded isoparametric shape functions from Eqn. (13), the strain components at any point on the shell midsurface can be expresse

$$\{\varepsilon\}=\sum_{i=1}^{8}\begin{bmatrix}\dfrac{1}{A_1}\dfrac{\partial N_i}{\partial \alpha_1} & \dfrac{N_i}{A_1A_2}\dfrac{\partial A_1}{\partial \alpha_2} & \dfrac{N_i}{R_1} & 0 & 0 \\ \dfrac{N_i}{A_1A_2}\dfrac{\partial A_2}{\partial \alpha_1} & \dfrac{1}{A_2}\dfrac{\partial N_i}{\partial \alpha_2} & \dfrac{N_i}{R_2} & 0 & 0 \\ \dfrac{1}{A_2}\dfrac{\partial N_i}{\partial \alpha_2}-\dfrac{N_i}{A_1A_2}\dfrac{\partial A_1}{\partial \alpha_2} & \dfrac{1}{A_1}\dfrac{\partial N_i}{\partial \alpha_1}-\dfrac{N_i}{A_1A_2}\dfrac{\partial A_2}{\partial \alpha_1} & \dfrac{2N_i}{R_{12}} & 0 & 0 \\ -\dfrac{1}{2}\dfrac{1}{R_{12}}\left(\dfrac{1}{A_2}\dfrac{\partial N_i}{\partial \alpha_2}+\dfrac{N_i}{A_1A_2}\dfrac{\partial A_1}{\partial \alpha_2}\right) & \dfrac{1}{2}\dfrac{1}{R_{12}}\left(\dfrac{1}{A_1}\dfrac{\partial N_i}{\partial \alpha_1}+\dfrac{N_i}{A_1A_2}\dfrac{\partial A_2}{\partial \alpha_1}\right) & 0 & \dfrac{1}{A_1}\dfrac{\partial N_i}{\partial \alpha_1} & \dfrac{N_i}{A_1A_2}\dfrac{\partial A_1}{\partial \alpha_2} \\ \dfrac{1}{2}\dfrac{1}{R_{12}}\left(\dfrac{1}{A_2}\dfrac{\partial N_i}{\partial \alpha_2}+\dfrac{N_i}{A_1A_2}\dfrac{\partial A_1}{\partial \alpha_2}\right) & -\dfrac{1}{2}\dfrac{1}{R_{12}}\left(\dfrac{1}{A_1}\dfrac{\partial N_i}{\partial \alpha_1}+\dfrac{N_i}{A_1A_2}\dfrac{\partial A_2}{\partial \alpha_1}\right) & 0 & \dfrac{N_i}{A_1A_2}\dfrac{\partial A_2}{\partial \alpha_1} & \dfrac{1}{A_2}\dfrac{\partial N_i}{\partial \alpha_2} \\ C_0\left(\dfrac{1}{A_2}\dfrac{\partial N_i}{\partial \alpha_2}+\dfrac{N_i}{A_1A_2}\dfrac{\partial A_1}{\partial \alpha_2}\right) & -C_0\left(\dfrac{1}{A_1}\dfrac{\partial N_i}{\partial \alpha_1}+\dfrac{N_i}{A_1A_2}\dfrac{\partial A_2}{\partial \alpha_1}\right) & 0 & \dfrac{1}{A_2}\dfrac{\partial N_i}{\partial \alpha_2}-\dfrac{N_i}{A_1A_2}\dfrac{\partial A_1}{\partial \alpha_2} & \dfrac{1}{A_1}\dfrac{\partial N_i}{\partial \alpha_1}-\dfrac{N_i}{A_1A_2}\dfrac{\partial A_2}{\partial \alpha_1}\end{bmatrix}\begin{Bmatrix}u_{0i}\\ v_{0i}\\ w_i\\ \theta_{1i}\\ \theta_{2i}\end{Bmatrix} \tag{56}$$

$$\{\varepsilon\}=\left[B_b^e\right]\{d^e\} \tag{57}$$

$\left[B_b^e\right]$ is the element in plane stain- displacement matrix and $C_o=\dfrac{1}{2}\left(\dfrac{1}{R_1}-\dfrac{1}{R_2}\right)$

4.2.2 Transverse strain displacement matrix

According to the FSDT, the transverse shear strain vector of a doubly curved shell element may be expressed as

$$\begin{Bmatrix}\gamma_{yz}\\ \gamma_{xz}\end{Bmatrix}=\begin{Bmatrix}\theta_2+\frac{1}{A_2}\frac{\partial w}{\partial \alpha_2}-\frac{u}{R_{12}}-\frac{v}{R_2}\\ \theta_1+\frac{1}{A_1}\frac{\partial w}{\partial \alpha_1}-\frac{u}{R_1}-\frac{v}{R_{12}}\end{Bmatrix} \tag{58}$$

And hence the transverse shear strain at any point on the shell mid surface can be expressed as

$$\begin{Bmatrix}\gamma_{yz}\\ \gamma_{xz}\end{Bmatrix}=\sum_{k=1}^{nd}\begin{bmatrix}-\frac{N_i}{R_{12}} & -\frac{N_i}{R_2} & \frac{1}{A_2}\frac{\partial N_i}{\partial \alpha_2} & 0 & N_i\\ -\frac{N_i}{R_1} & -\frac{N_i}{R_{12}} & \frac{1}{A_1}\frac{\partial N_i}{\partial \alpha_1} & N_i & 0\end{bmatrix}\begin{Bmatrix}u_{0i}\\ v_{0i}\\ w_i\\ \theta_{1i}\\ \theta_{2i}\end{Bmatrix} \tag{59}$$

$$\begin{Bmatrix}\gamma_{yz}\\ \gamma_{xz}\end{Bmatrix}=\left[B_s^e\right]\left\{d^e\right\} \tag{60}$$

$\left[B_s^e\right]$ is the element transverse stain- displacement matrix.

4.2.3 ABBD matrix

The resultant force per unit width is

$$\{N\}=\begin{bmatrix}N_{xx} & N_{yy} & N_{xy}\end{bmatrix}^T \tag{61}$$

The resultant moment per unit width is

$$\{M\}=\begin{bmatrix}M_{xx} & M_{yy} & M_{xy}\end{bmatrix}^T \tag{62}$$

In plane strains of mid-surface is

$$\left\{\varepsilon^0\right\}=\begin{bmatrix}\varepsilon_{xx}^0 & \varepsilon_{yy}^0 & \gamma_{xy}^0\end{bmatrix}^T \tag{63}$$

Curvatures of mid-surface is

$$\{k\}=\begin{bmatrix}k_{xx} & k_{yy} & k_{xy}\end{bmatrix}^T \tag{64}$$

The strain at any point on an element

$$\{\varepsilon\}^{(xy)}=\left\{\varepsilon^0\right\}+z\{k\} \tag{65}$$

The resultant force per unit width can be expressed as

$$\begin{aligned}\{N\}&=\int_{-h/2}^{h/2}\{\sigma\}^{(xy)}\,dz\\ \{N\}&=[A]\left\{\varepsilon^0\right\}+[B]\{k\}\end{aligned} \tag{66}$$

The resultant moment per unit width

$$\{M\} = \int_{-h/2}^{h/2} \{\sigma\}^{(xy)}\, z dz$$
$$\{M\} = [B]\varepsilon_o + [D]k \tag{67}$$

Eqs. (37) and (38) can be expressed in matrix form as

$$\begin{Bmatrix} \{N\} \\ \{M\} \end{Bmatrix} = \begin{bmatrix} [A] & [B] \\ [B] & [D] \end{bmatrix} \begin{Bmatrix} \{\varepsilon^0\} \\ \{k\} \end{Bmatrix} \tag{68}$$

$$\{\sigma\} = \begin{bmatrix} [A] & [B] \\ [B] & [D] \end{bmatrix} \{\varepsilon\} \tag{69}$$

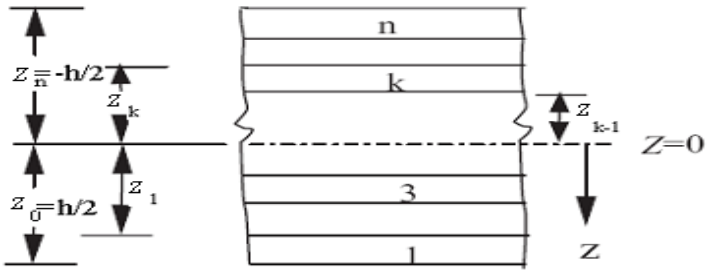

FIGURE 4-3 STACKING SEQUENCE IN LAMINATE

$$[Q_b]_k = \begin{bmatrix} Q_{11} & Q_{12} & 0 \\ Q_{12} & Q_{22} & 0 \\ 0 & 0 & Q_{66} \end{bmatrix} \tag{70}$$

$$Q_{11} = \frac{E_1}{1-\nu_{12}\nu_{21}} \tag{71}$$

$$Q_{22} = \frac{E_2}{1-\nu_{12}\nu_{21}} \tag{72}$$

$$Q_{12} = \frac{\nu_{12}E_2}{1-\nu_{12}\nu_{21}} = \frac{\nu_{21}E_1}{1-\nu_{12}\nu_{21}} \tag{73}$$

$$Q_{66} = G_{12} \tag{74}$$

$$\frac{\nu_{12}}{E_1} = \frac{\nu_{21}}{E_2} \tag{75}$$

$$\nu_{12} = -\frac{\varepsilon_2}{\varepsilon_1} \tag{76}$$

$$\nu_{21} = -\frac{\varepsilon_1}{\varepsilon_2} \tag{77}$$

The transformation matrix

$$[R_T]_k^{-1} = \begin{bmatrix} \cos^2\theta & \sin^2\theta & -2\sin\theta\cos\theta \\ \sin^2\theta & \cos^2\theta & 2\sin\theta\cos\theta \\ \sin\theta\cos\theta & -\sin\theta\cos\theta & \cos^2\theta - \sin^2\theta \end{bmatrix} \tag{78}$$

The transformed elasticity matrix for bending

$$\left[\overline{Q_b}\right]_k = [R_T]_k^{-1}[Q_b]_k[R_T]_k^{-T} \tag{79}$$

$$[Q_S]=\begin{bmatrix} KG_{23} & 0 \\ 0 & KG_{13} \end{bmatrix} \tag{80}$$

Where K denotes shear correction factor

The transformation matrix

$$[R_s]=\begin{bmatrix} \cos\theta & -\sin\theta \\ \sin\theta & \cos\theta \end{bmatrix} \tag{81}$$

The transformed elasticity matrix for transverse shear

$$\left[\overline{Q}_s\right]=[R_s]^T[Q_S][R_s] \tag{82}$$

$$\left[\overline{D}_s\right]=\sum_{k=1}^{n}\left[\overline{Q}_s\right](Z_k-Z_{k-1}) \tag{83}$$

The extensional stiffness matrix

$$[A]=\sum_{k=1}^{n}\left[\overline{Q_b}\right]_k\left(Z_k-Z_{k-1}\right) \tag{84}$$

The extensional-bending coupling stiffness matrix

$$[B]=\frac{1}{2}\sum_{k=1}^{n}\left[\overline{Q_b}\right]_k\left(Z_k^2-Z_{k-1}^2\right) \tag{85}$$

The bending stiffness matrix

$$[D]=\frac{1}{3}\sum_{k=1}^{n}\left[\overline{Q_b}\right]_k\left(Z_k^3-Z_{k-1}^3\right) \tag{86}$$

4.3 Equation of motion

The elastic finite element formulation has been derived for static and dynamic analysis.

4.3.1 Static finite equations

The total potential energy of the element is given by

$$\prod = U - W \tag{87}$$

U and W are the strain energy of the entire structure and work done by the external force.

Strain energy of the shell structure is given by,

$$\begin{aligned} U &= \frac{1}{2}\int_V \{\varepsilon\}^T\{\sigma\}dV \\ U &= \frac{1}{2}\int_V \{\varepsilon\}^T[C]\{\varepsilon\}dV \\ U &= \frac{1}{2}\{d^e\}^T\int_V\left[B_u^e\right]^T[C]\left[B_u^e\right]dV\{d^e\} \\ U &= \frac{1}{2}\{d^e\}^T\left[K_{uu}^e\right]\{d^e\} \end{aligned} \tag{88}$$

Work done by external force is given by,

$$W = \int_{A_1} \left\{d^e\right\}^T \left\{ f_s^e(x,y)\right\} dA$$

$$W = \left\{d^e\right\}^T \int_{A_1} \left[N\right]^T \left\{ f_s^e(x,y)\right\} dA \tag{89}$$

$$W = \left\{d^e\right\}^T \left\{F^e\right\}$$

Substituting the values of U and W in total potential energy Eqn.58, we have

$$\left[K_{uu}^e\right]\left\{d^e\right\} = \left\{F^e\right\} \tag{90}$$

Eqn. (61) is the elastic equation for one element.

Where,

$\left[K_{uu}^e\right]$ is the element structural stiffness matrix is given by

$$\left[K_{uu}^e\right] = \int_V \left[B_u^e\right]^T [C] \left[B_u^e\right] dV \tag{91}$$

$$\left[K_{uu}^e\right] = \left[K_{bb}^e\right] + \left[K_{ss}^e\right] \tag{92}$$

$$\left[B_u^e\right] = \begin{bmatrix} \left[B_b^e\right] & [0] \\ [0] & \left[B_s^e\right] \end{bmatrix} \tag{93}$$

$$[C] = \begin{bmatrix} [D_b] & [0] \\ [0] & [D_s] \end{bmatrix} \tag{94}$$

$[D_b]$ is the in-plane/bending constitutive matrix and $[D_s]$ is the transverse shear constitutive matrix.

$\left[K_{bb}^e\right]$, is the element in plane/bending stiffness matrix.

$$\left[K_{bb}^e\right] = \int_V \left[B_b^e\right]^T [D_b] \left[B_b^e\right] dV$$

$$\left[K_{bb}^e\right] = \int_\Omega \left[B_b^e\right]^T \begin{bmatrix} [A] & [B] \\ [B] & [D] \end{bmatrix} \left[B_b^e\right] d\Omega \tag{95}$$

$\left[K_{ss}^e\right]$, is the element transverse shear stiffness matrix

$$\left[K_{ss}^e\right] = \int_V \left[B_s^e\right]^T [D_s] \left[B_s^e\right] dV$$

$$\left[K_{ss}^e\right] = \int_\Omega \left[B_s^e\right]^T \left[\overline{D}_s\right] \left[B_s^e\right] d\Omega \tag{96}$$

$\left\{F^e\right\}$, is the element external mechanical force vector

$$\left\{F^e\right\} = \int_A \left[N\right]^T \left\{ f_s^e(x,y)\right\} dA \tag{97}$$

Hence all the element stiffness matrices can be expressed in its final form as

$$\left[K^e\right]=\int_{-1}^{1}\int_{-1}^{1}\left[K_h^e\right]|J|d\xi d\eta \tag{98}$$

After assembling the elemental stiffness matrices, the global set of elastic equations is given by

$$\left[K_{uu}\right]\{d\}=\{F\} \tag{99}$$

4.3.2 Dynamic finite equations

The dynamic finite element formulation has been derived by using Hamilton's principle as

$$\int_{t_1}^{t_2}(\delta L+\delta W)dt=0 \tag{100}$$

where, the Lagrangian, $L=T-U$

T is the kinetic energy of the system, U is the elastic strain energy, W is the external work done by the force on the structure.

$$\int_{t_1}^{t_2}\left(\delta\left[T-U\right]+\delta W\right)dt=0 \tag{101}$$

where t_1 and t_2 defines the time interval.

Kinetic energy T is given by,

$$T=\int_V\rho\left(\frac{1}{2}\{\dot{d}\}^T\{\dot{d}\}\right)dV \tag{102}$$

ρ is the mass density.

Individual parts of the Hamilton equation can be written as follows:

Part 1: The kinetic energy of the system

$$\int_{t_1}^{t_2}\delta T dt=\delta\int_{t_1}^{t_2}\int_V\rho\left(\frac{1}{2}\{\dot{d}\}^T\{\dot{d}\}\right)dVdt$$

$$\int_{t_1}^{t_2}\delta T dt=-\int_{t_1}^{t_2}\int_V\rho\{\delta d\}^T\{\ddot{d}\}dVdt$$

$$\int_{t_1}^{t_2}\delta T dt=-\int_{t_1}^{t_2}\{\delta d^e\}^T\left[\int_V\rho\left[N^T\right][N]dV\right]\{\ddot{d}^e\}dt$$

$$\int_{t_1}^{t_2}\delta T dt=-\int_{t_1}^{t_2}\{\delta d^e\}^T\left[M_{uu}^e\right]\{\ddot{d}^e\}dt \tag{103}$$

Part 2: The total internal energy of the system

$$\int_{t1}^{t2}\delta U dt=\int_{t1}^{t2}\delta V^m dt\ \int_{t1}^{t2}\delta U dt=\int_{t1}^{t2}\left(\{\delta d^e\}^T\left[K_{uu}^e\right]\{d^e\}\right)dt \tag{104}$$

Part 3: The work done by the external forces

$$\int_{t_1}^{t_2} \delta W_e dt = \int_{t_1}^{t_2} \left[\int_{A_1} \left\{ \delta d^e \right\}^T \left\{ f_s^e (x,y) \right\} dA \right] dt$$

$$\int_{t_1}^{t_2} \delta W_e dt = \int_{t_1}^{t_2} \left[\left\{ \delta d^e \right\}^T \int_{A_1} [N]^T \left\{ f_s^e (x,y) \right\} dA \right] dt$$

$$\int_{t_1}^{t_2} \delta W_e dt = \left\{ \delta d^e \right\}^T \left\{ F^e \right\} \tag{105}$$

Substituting eqns. (74), (75), (76) in eq. (71) gives

$$\int_{t_1}^{t_2} \left[\left\{ \delta d^e \right\}^T \left(-\left[M_{uu}^e \right] \left\{ \ddot{d}^e \right\} - \left[K_{uu}^e \right] \left\{ d^e \right\} + \left\{ F^e \right\} \right) \right] dt = 0 \tag{106}$$

Since $\left\{ \delta d^e \right\}$ can be any arbitrary values, $\left\{ \delta d^e \right\} \neq 0$ and therefore the eq. (43) is zero only if

$$\left[M_{uu}^e \right] \left\{ \ddot{d}^e \right\} + \left[K_{uu}^e \right] \left\{ d^e \right\} = \left\{ F^e \right\} \tag{107}$$

Eqn. (78) is dynamic finite element equations of one element.

Where the structural mass matrix is given by,

$$\left[M_{uu}^e \right] = \int_V \rho \left[N^T \right] [N] dV \tag{108}$$

The displacement at any point in the laminate cane be expressed as

$$\begin{Bmatrix} u \\ v \\ w \end{Bmatrix} = \begin{Bmatrix} u_0 - z\theta_x \\ v_0 - z\theta_y \\ w \end{Bmatrix} \tag{109}$$

$$\begin{Bmatrix} u \\ v \\ w \end{Bmatrix} = \sum_{i=1}^{nd} \begin{bmatrix} N_i & 0 & 0 & -zN_i & 0 \\ 0 & N_i & 0 & 0 & -zN_i \\ 0 & 0 & N_i & 0 & 0 \end{bmatrix} \begin{Bmatrix} u_{0i} \\ v_{0i} \\ w_i \\ \theta_{xi} \\ \theta_{yi} \end{Bmatrix} \tag{110}$$

$$\begin{Bmatrix} u \\ v \\ w \end{Bmatrix} = [N] \left\{ d^e \right\} \tag{111}$$

$$\left[M_{uu}^e \right] = \int_V \rho \left[N^T \right] [N] dV \tag{112}$$

$$\left[M_{uu}^e \right] = \int_\Omega \int_{-\frac{h}{2}}^{\frac{h}{2}} \rho \left[N^T \right] [N] dz d\Omega \tag{113}$$

Mass matrix in its final form can be expressed as

$$\left[M_{uu}^{e}\right]=\int_{-1}^{1}\int_{-1}^{1}\int_{-h/2}^{h/2}\rho\left[N\right]^{T}\left[N\right]dz\left|J\right|d\xi d\eta \tag{114}$$

4.4 Calculation of non-dimensional frequencies

In order to verify the above formulation for spherical shell having mesh 10×10, the various non-dimensional frequencies of the present formulation are compared with existing ones.

$$\omega^{**}=\omega\frac{a^{2}}{h}\sqrt{\frac{\rho}{E_{2}}} \tag{115}$$

Where ω^{**} is the non-dimensional frequency, ω is the natural frequency, a is the length of shell structure along x-axis, h is the thickness of the laminate, ρ is the density of composite, E_2 is the transverse modulus of the lamina having 0^0 orientation.

4.5 State space method for impulse response

The equation of motion of system considering damping in modal form is given as:

$$\left\{\ddot{\gamma}_i\right\}+\left[2\zeta_i\omega_i\right]\left\{\dot{\gamma}_i\right\}+\left[\omega_i^{2}\right]\left\{\gamma_i\right\}=\left\{f_i\right\} \tag{116}$$

Where $\gamma_i,\zeta_i,\omega_i$ *and* f_i are the modal coordinates, modal damping ratio, natural frequency and force vector in modal form for i=1, 2, 3…., dof.

For damped systems which are modeled using Rayleigh proportional damping, it is difficult to determine the Rayleigh constants. Calculating Rayleigh damping coefficients for large degree of freedom system has been provided with detail in Chowdhury and Dasgupta [21]. Assuming 3% of the total modes to be active modes or which participate in mass proportional damping. As there is no data regarding the damping ratios for the above formulated hybrid composite we proceed the investigation by assuming the damping ratio of the first mode to be 0.01 and damping ratio of the last active mode to be 0.05. The constants α and β can be calculated using the damping ratios and natural frequencies of the first mode and the last active mode. The damping ratio for the i^{th} intermediate mode ζ_i can be calculated once the value of α and β are known. Thus

$$\zeta_i=\frac{\alpha}{2\omega_i}+\beta\omega_i \tag{117}$$

The state space and output equations in modal form for *n* number of modes can be written as,

$$\begin{Bmatrix} \dot{\chi}_1 \\ \vdots \\ \dot{\chi}_{2n} \end{Bmatrix} = \begin{bmatrix} (0)_{n\times n} & (I)_{n\times n} \\ -\left(\omega_n^2\right)_{n\times n} & -\left(2\zeta_n\omega_n\right)_{n\times n} \end{bmatrix} \begin{Bmatrix} \chi_1 \\ \vdots \\ \chi_{2n} \end{Bmatrix} + \begin{bmatrix} (0)_{dof\times 1} \\ -\psi^T_{dof\times dof} \times M^{-1}_{dof\times dof} \end{bmatrix} \left\{ \psi^T_{dof\times dof} \times F_{dof\times 1} \right\} \quad (118)$$

$$\begin{Bmatrix} \gamma_1 \\ \vdots \\ \gamma_{2n} \end{Bmatrix} = [I]_{2n\times 2n} \begin{Bmatrix} \chi_1 \\ \vdots \\ \chi_{2n} \end{Bmatrix} + [0]_{2n\times 2n} \left\{ \psi^T_{dof\times dof} \times F_{dof\times 1} \right\} \quad (119)$$

Where $(0)_{n\times n}$ is null matrix, $(I)_{n\times n}$ is the identity matrix, $\left(\omega_n^2\right)_{n\times n}$ and $\left(2\zeta_n\omega_n\right)_{n\times n}$ are diagonal matrices, $\chi_{1.....}\chi_{2n}$ are the state vectors.

5

RESULTS AND DISCUSSION

Summary of the above chapters

Hybrid composite is a composite which consists of nanoparticles to enhance the strength as compared to conventional composites. A model has been proposed to determine the elastic properties of hybrid composite. The hybrid composite consists of conventional fiber and nanocomposite as matrix. The first step here is to determine the properties of nanocomposite which is done by using Mori – Tanaka method. The CNTs are considered as cylindrical inclusions in polymer matrix in Mori – Tanaka method. Assuming perfect bonding between carbon fibers and nanocomposite matrix, the effective properties of the hybrid composite has been evaluated using mechanics of materials approach.

An 8 noded shell element has been used for the finite element analysis having 5 degrees of freedom each node $\left(u, v, w, \theta_x, \theta_y\right)$. A 10×10 finite element mesh has been used to model the shell element. The shell coordinates which are in Cartesian form are converted into parametric form using two parameters $\left(\alpha_1, \alpha_2\right)$. These parameters are again mapped into isoparametric form $\left(\eta, \xi\right)$. A 16 layered laminate with stacking sequence $[0\ -45\ 45\ 90]_{2S}$ has been used for vibration analysis of simply supported shell element. The dynamic equations of shell are derived using Hamilton's principle. As the damping characters of the dynamic system are not available, for further investigation damping ratio of first mode and last active mode are assumed. Using Rayleigh damping the damping ratios of intermediate modes can be calculated. The time decay of the system from maximum amplitude to 5% of the maximum amplitude has been used as a parameter to study various shell structures by varying the volume fraction of CNTs in nanocomposite and by varying carbon fiber volume fraction.

Validation of formulation

Free vibration analysis is done to validate the above formulation. A 2, 3 and 4 layered cross ply laminate has been used to carry out free vibration analysis by varying the a/h ratio and R/a ratio of the spherical shell.

Reference [23]

Panel	a/h	R/a							
		1	2	5	10	20	50	100	500
0/90	10	14.481	10.749	9.2302	8.9841	8.9212	8.9035	8.9009	8.9001
0/90	100	125.93	67.369	28.826	16.706	11.841	10.063	9.7825	9.6873
0/90/0	10	16.115	13.382	12.372	12.215	12.176	12.165	12.163	12.162
0/90/0	100	125.99	68.075	30.993	20.347	16.627	15.424	15.244	15.183
0/90/90/0	10	16.172	13.447	12.437	12.280	12.240	12.229	12.228	12.226
0/90/90/0	100	126.33	68.294	31.079	20.38	16.638	15.426	15.245	15.184

TABLE 5-1 NON-DIMENSIONAL FREQUENCY [REF:23]

Present Formulation

Panel	a/h	R/a							
		1	2	5	10	20	50	100	500
0/90	10	15.51217	11.1521	8.906713	8.373873	8.166252	8.061078	8.027878	7.990367
0/90	100	136.0635	73.90925	31.89584	18.20593	12.12838	9.353029	8.72118	8.358714
0/90/0	10	15.5545	12.22585	11.01655	10.82998	10.78238	10.76802	10.7647	10.75471
0/90/0	100	142.7383	76.47821	32.7317	19.15716	13.78834	11.85253	11.54031	11.43834
0/90/90/0	10	14.8861	11.99612	10.95903	10.79977	10.75936	10.74652	10.74316	10.73102
0/90/90/0	100	134.838	72.67357	31.29011	18.50931	13.52047	11.74193	11.45988	11.35508

TABLE 5-2 NON-DIMENSIONAL FREQUENCY FOR THE PRESENT FORMULATION

Material Properties

Properties of various constituents of Hybrid composite

Constituent	C_{11}(GPa)	C_{12}(GPa)	C_{22}(GPa)	C_{23}(GPa)	C_{55}(GPa)	Density(kg/m^3)
Carbon fiber[22]	236.4	10.6	24.8	10.7	25	1800[24]
(25,25), 5 walled CNT[6]	1180	146	411	133	189	1740[25]
Epoxy[18]	13.4615	5.7692	13.4615	5.7692	3.8462	1150

TABLE 5-3 MATERIAL PROPERTIES OF VARIOUS CONSTITUENTS IN HYBRID COMPOSITE

C11

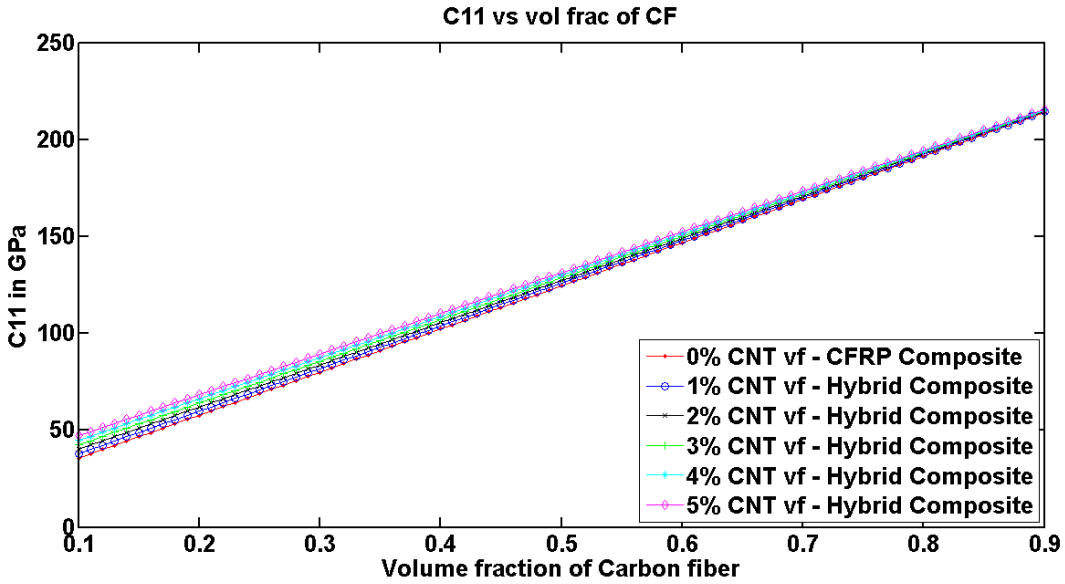

FIGURE 5-1 VARIATION OF C_{11} W.R.T VARIATION OF CARBON FIBER AND CNT VOLUME FRACTION

From Fig. 5.1, it can be seen that as the carbon fiber volume fraction increases the longitudinal elastic properties increase. At lower volume fractions of carbon fiber (10%) it can be observed that for CFRP composite the elastic modulus is around 35GPa, but with the increase in volume fraction of CNT from 1% to 5% the elastic modulus has increased from 38GPa to 47.3GPa. With the increase in carbon fiber volume fraction, the volume fraction of nanocomposite goes on decreasing; as a result the elastic properties almost converge at higher volume fractions of carbon fiber.

C12 and C23

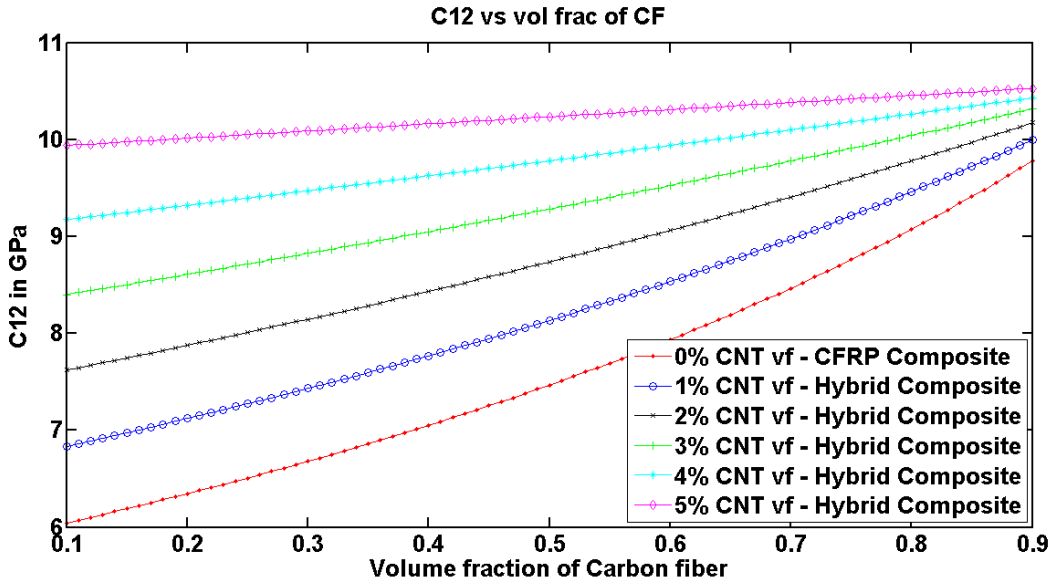

FIGURE 5-2 VARIATION OF C_{12} W.R.T VARIATION OF CARBON FIBER AND CNT VOLUME FRACTION

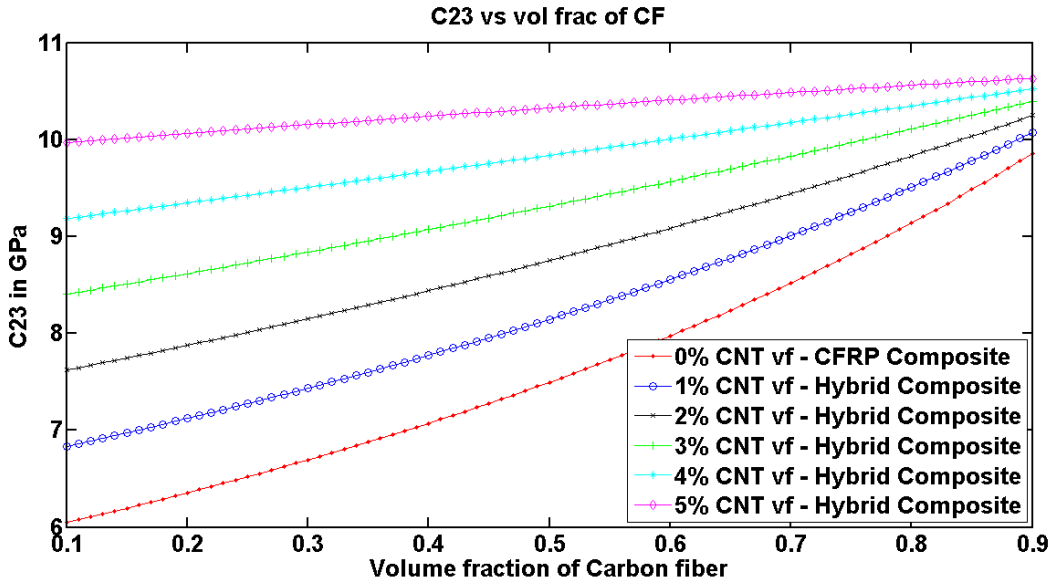

FIGURE 5-3 VARIATION OF C_{23} W.R.T VARIATION OF CARBON FIBER AND CNT VOLUME FRACTION

From Fig. 5.2 and Fig. 5.3, similarly as C11, the elastic properties along 1-2 direction also increase with the increase with in volume fraction of carbon fiber. At lower volume fractions (10%) it can be observed that CFRP has elastic modulus of 6Gpa, but with increase in CNT volume fraction from 1% to 5%, the elastic properties have increased from 6.8Gpa to 10Gpa. With the increase in carbon fiber volume fraction, it can be observed that composites having lower CNT volume fractions show steep increase in elastic properties than compared to composites having higher CNT volume fractions.

C22

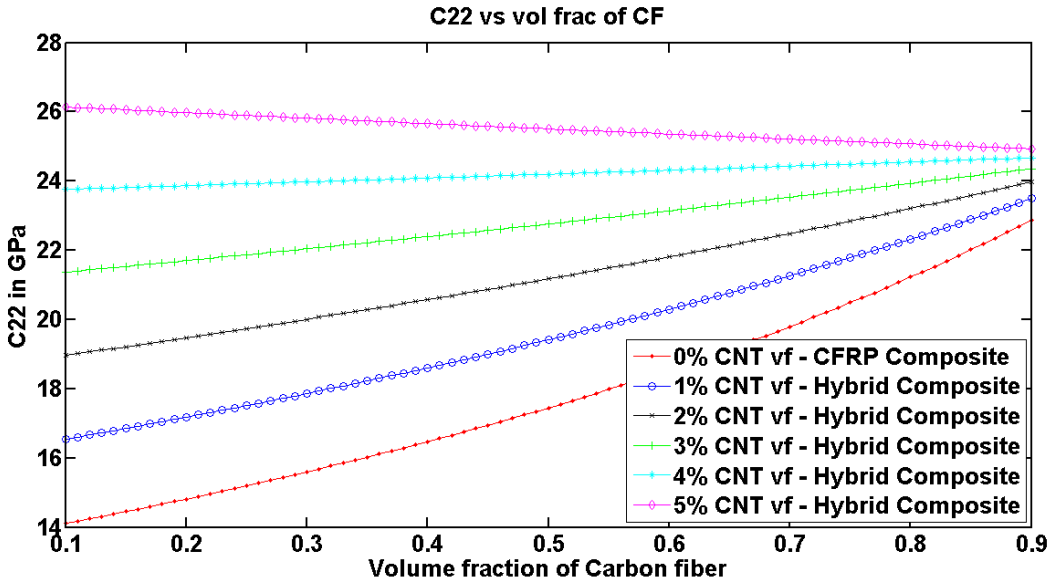

FIGURE 5-4 VARIATION OF C_{22} W.R.T VARIATION OF CARBON FIBER AND CNT VOLUME FRACTION

From Fig. 5.4, it can be seen that the transverse elastic properties have improved with the addition of CNT in matrix material for lower volume fractions of carbon fiber. This increase in elastic properties can be attributed to the randomly distributed CNTs. With the increase in carbon fiber volume fraction the composites having lower volume fractions of CNT have shown an increase in transverse elastic modulus, but for composites having higher volume fractions of CNT with the increase in carbon fiber volume fraction there is decrease in transverse elastic modulus.

C55

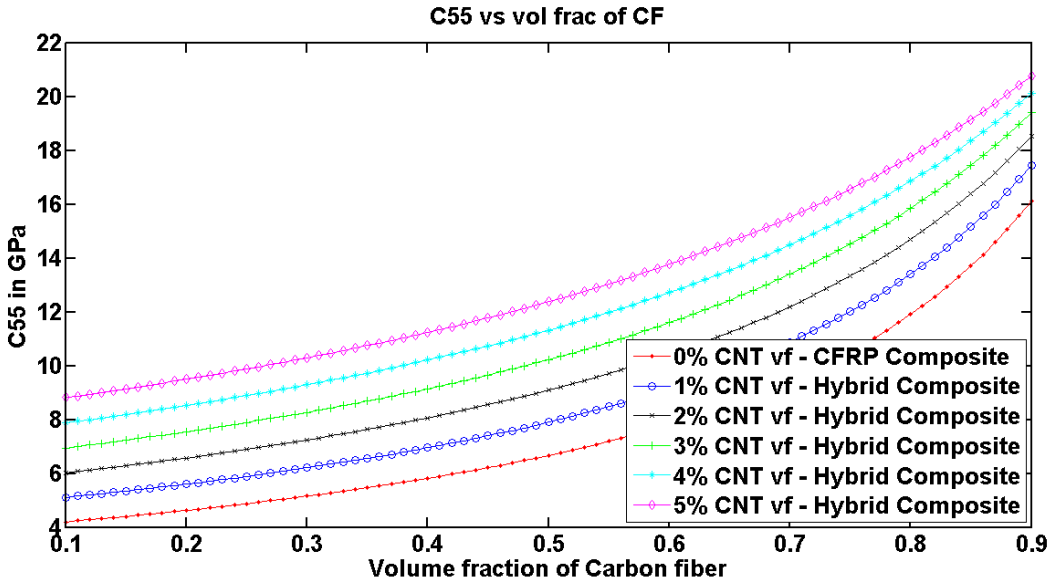

FIGURE 5-5 VARIATION OF C_{55} W.R.T VARIATION OF CARBON FIBER AND CNT VOLUME FRACTION

From Fig. 5.5, it can be observed that the in-plane shear properties have increased with increase in volume fractions of CNT and carbon fiber. Composites normally fail due to shear. So in order avoid failure it is advantageous to use hybrid composite in place of conventional CFRP composites.

Impulse response

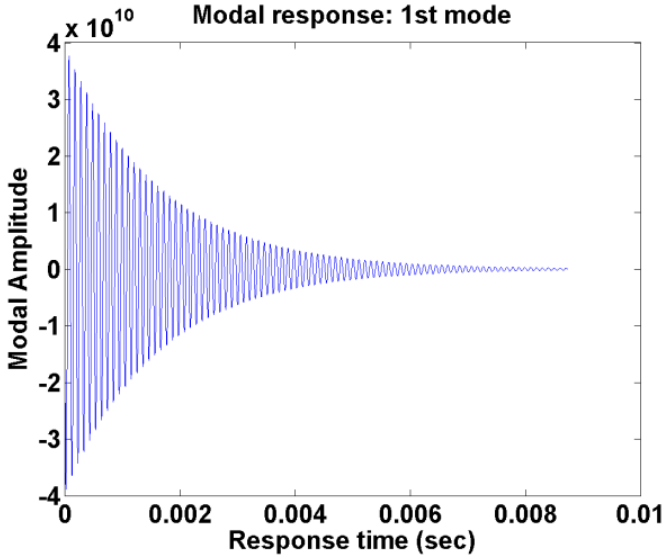

FIGURE 5-6 IMPULSE RESPONSE OF CFRP COMPOSITE FOR THICK PLATE

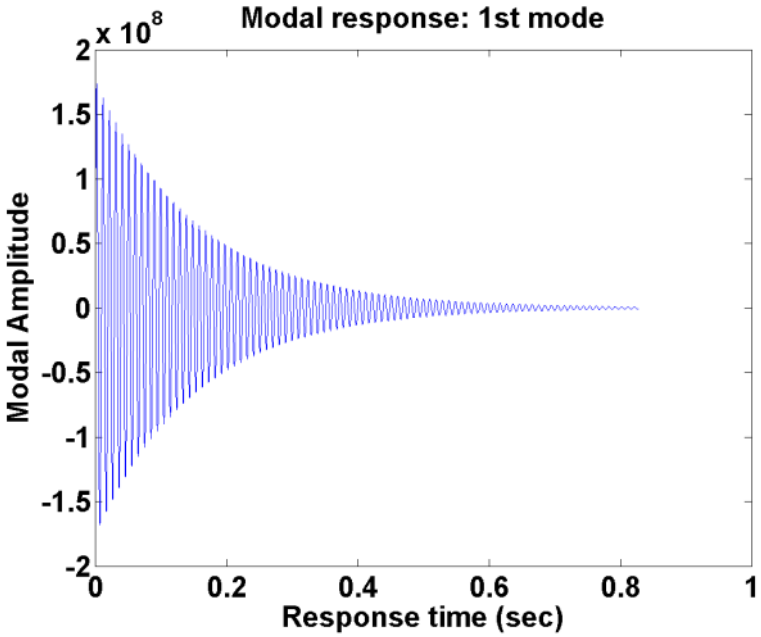

FIGURE 5-7 IMPULSE RESPONSE OF CFRP COMPOSITE FOR THIN PLATE

Fig. 5.6 and Fig. 5.7 indicate the response of thick plate and thin plate in modal coordinates for the first mode of vibration.

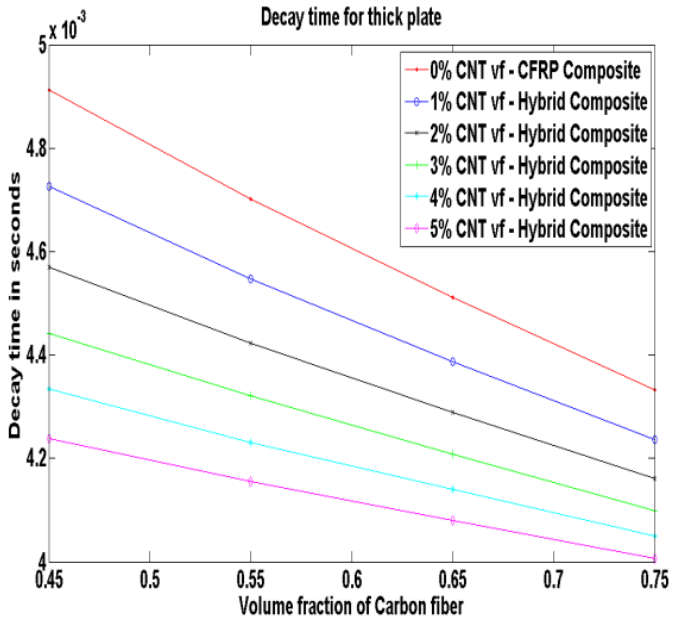

FIGURE 5-8 DECAY TIME FOR THICK PLATE BY VARYING THE CNT VOLUME FRACTIONS FOR DIFFERENT VOLUME FRACTIONS OF CARBON FIBER

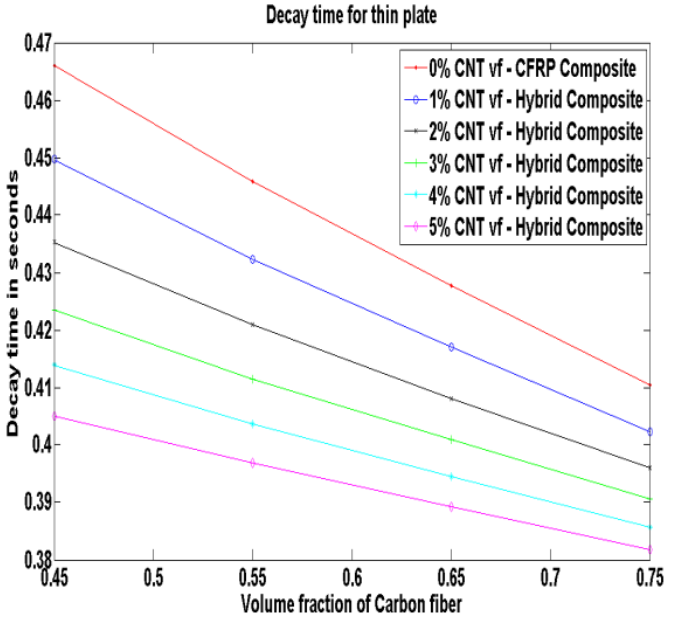

FIGURE 5-9 DECAY TIME FOR THIN PLATE BY VARYING THE CNT VOLUME FRACTIONS FOR DIFFERENT VOLUME FRACTIONS OF CARBON FIBER

Fig. 5.8 and Fig. 5.9 show the decay time for thick and thin plates. At lower volume fractions carbon fiber, the decay time of the system goes on decreasing with increase in CNT volume fraction. As the volume fraction of carbon fiber increases the decay time also decreases.

6

CONCLUSION

This chapter presents important observations on the material properties, Rayleigh damping in composite materials, impulse response, and decay time.

Conclusions

The hybrid composite has been modeled using Mori-Tanaka method and mechanics of materials method. It is found that

1. The longitudinal properties C11 of the hybrid composite increase with the increase in volume fraction of CNT at lower volume fractions of carbon fiber. As the volume fraction of carbon fiber goes on increasing the longitudinal modulus tends to converge because the volume fraction of CNT goes on decreasing.
2. There is tremendous increase in elastic properties C12 and C23 of the hybrid composite with the increase in volume fraction of CNT at lower volume fractions of carbon fiber. As the volume fractions of carbon fiber goes on increasing there is slow increase in composites having higher volume fractions of CNT as compared to composites having lower volume fractions of CNTs.
3. The transverse modulus C_{22} of the hybrid increases with the increase in CNT volume fraction but as the volume fraction of carbon fiber increases the composites having lower CNT volume fractions show increase in transverse modulus and composites having higher CNT volume fraction show gradual decrease in transverse modulus.
4. The in-plane shear modulus C_{55} increases with increase in CNT and carbon fiber volume fraction.
5. The amplitude goes on decreasing with increase in damping ratio.
6. As the volume fraction of CNT increases the decay time goes on decreasing.
7. The decay time of thick plate is less than the decay time of thin plate.

Future Scope

- Estimate temperature dependent and hygrothermal properties.
- Buckling analysis of hybrid composite laminated shell structure.
- Active vibration control of the laminated shell structure.
- Delamination analysis.
- Nonlinear analysis of laminated shell structure.

REFERENCES:

[1]. Usuki et al, Inorganic Polymeric Nanocomposites and Membranes Advances in Polymer Science Volume 179, 2005, pp 135-195.

[2]. R.C.L. Dutra, B.G. Soaresb, E.A. Campos, J.L.G. Silva, Hybrid composites based on polypropylene and carbon fiber and epoxy matrix, Polymer 41, 2000, pp 3841–3849.

[3]. Timoshenkho and Krieger, Theory of Plates and Shells, McGraw Hill Publication.

[4]. Ronald F. Gibson, Modal vibration response measurements for characterization of composite materials and structures, Composites Science and Technology 60, 2000, pp: 2769-2780

[5]. R. Chandra 1, S.P. Singh, K. Gupta, Damping studies in fiber-reinforced composites - a review, Composite Structures 46, 1999, pp 41-51

[6]. J.P. Lu, Elastic properties of carbon nanotubes and nanoropes, Physical Review Letters vol. 79, 1997, pp. 1297–300

[7]. Mohammad A. Rafiee, Javad Rafiee, Zhou Wang, Huaihe Song, Zhong-Zhen Yu, and Nikhil Koratkar, Enhanced Mechanical Properties of Nanocomposites at Low Graphene Content, American Chemical Society – NANO, Vol. 3, No. 12, 2009, pp 3884–3890

[8]. F.H. Gojny, M.H.G. Wichmann, U. Koepke, B. Fiedler, K. Schulte, Carbon nanotube-reinforced epoxy-composites: enhanced stiffness and fracture toughness at low nanotube content, Composites Science and Technology 64, pp: 2363–2371, 2004

[9]. Florian H. Gojny 1, Malte H.G. Wichmann, Bodo Fiedler, Karl Schulte, Influence of different carbon nanotubes on the mechanical properties of epoxy matrix composites – A comparative study, Composites Science and Technology 65, pp: 2300–2313, 2005

[10]. Gary D. Seidel, Dimitris C. Lagoudas, Micromechanical analysis of the effective elastic properties of carbon nanotube reinforced composites, Mechanics of Materials 38, pp: 884–907, 2006

[11]. Y.J. Liu, X.L. Chen, Evaluations of the effective material properties of carbon nanotube-based composites using a nanoscale representative volume element, Mechanics of Materials 35,pp: 69–81, 2003

[12]. R.B. Mathur, Sourav Chatterjee, B.P. Singh, Growth of carbon nanotubes on carbon fibre substrates to produce hybrid/phenolic composites with improved mechanical properties, Composites Science and Technology 68, pp: 1608–1615, 2008

[13]. Enrique J. Garcia, Brian L. Wardle, A. John Hart, Namiko Yamamoto, Fabrication and multifunctional properties of a hybrid laminate with aligned carbon nanotubes grown In Situ, Composites Science and Technology 68, pp: 2034‑2041, 2008

[14]. S. I. Kundalwal, M. C. Ray, Micromechanical analysis of fuzzy fiber reinforced composites, Int J Mech Mater Des 7,pp: 149–166, 2011

[15]. Tarapada Roy, DebabrataChakraborty, Optimal vibration control of smart fiber reinforced composite shell structures using improved genetic algorithm, Journal of Sound and Vibration 319, pp: 15–40, 2009

[16]. C. Kyriazoglou, F.J. Guild, Finite element prediction of damping of composite GFRP and CFRP laminates – a hybrid formulation – vibration damping experiments and Rayleigh damping, Composites Science and Technology 67, pp: 2643–2654, 2007

[17]. R. Verdejo, R. Stämpfli, M. Alvarez-Lainez, S. Mourad, M.A. Rodriguez-Perez, P.A. Brühwiler,M. Shaffer, Enhanced acoustic damping in flexible polyurethane foams filled with carbon nanotubes, Composites Science and Technology 69,pp: 1564‑1569, 2009

[18]. M.H. Yas, M. Heshmati, Dynamic analysis of functionally graded nanocomposite beams reinforced by randomly oriented carbon nanotube under the action of moving load, Applied Mathematical Modelling 36, pp: 1371–1394, 2012

[19]. JiangYu Li and Martin L. Dunn, Anisotropic coupled field inclusion and inhomogeneity problems, PHILOSOPHICAL MAGAZINE A, 1998, VOL. 77, and No. 5, 1341 – 1350.

[20]. Dong-Li Shi, Xi-Qiao Feng, Yonggang Y. Huang, Keh-Chih Hwang, Huajian Gao, The Effect of Nanotube Waviness and Agglomeration on the Elastic Property of Carbon Nanotube- Reinforced Composites, JOURNAL OF ENGINEERING MATERIALS AND TECHNOLOGY, Vol. 126, JULY 2004, pp: 250 – 257

[21]. Indrajit Chowdhury, Shambhu P. Dasgupta, Computation of Rayleigh Damping Coefficients for Large Systems, Department of Civil Engineering, Indian Institute of Technology.

[22]. Kuniaki Honjo, Thermal stresses and effective properties calculated for fiber composites using actual cylindrically-anisotropic properties of interfacial carbon coating, Carbon 45, 2007, pp:865–872

[23]. Tarapada Roy, P.Manikandan , DebabrataChakraborty, Improved shell finite element for piezothermoelastic analysis of smart fiber reinforced composite structures, Finite Elements in Analysis and Design 46, pp:710–720, 2010

[24]. Akihiro Mizutani, Yoshitake Nishi, Improved Strength in Carbon Fiber Reinforced Plastics due after Electron Beam Irradiation, Materials Transactions, Vol. 44, No. 9, pp. 1857 to 1860, The Japan Institute of Metals, 2003.

[25]. S.H. Kim, G.W. Mulholland, M.R. Zachariah, Density measurement of size selected multiwalled carbon nanotubes by mobility-mass characterization, Carbon (47), pp:1297-1302, 2009